

## Supporting Information

### PSMA-targeted melanin-like nanoparticles as a multifunctional nanoplatfom for prostate cancer theranostics

Liqun Dai,<sup>†a</sup> Guohua Shen,<sup>†a</sup> Peng Yang,<sup>b</sup> Yuanyuan Wang <sup>\*c</sup> and Zhenhua Liu <sup>\*d</sup>

<sup>a</sup> Department of Nuclear Medicine, Laboratory of Clinical Nuclear Medicine, West China Hospital, Sichuan University, Chengdu, 610041, China.

<sup>b</sup> College of Polymer Science and Engineering, State Key Laboratory of Polymer Materials Engineering, Sichuan University, Chengdu, 610065, China.

<sup>c</sup> Department of Endocrine and Breast Surgery, The First Affiliated Hospital of Chongqing Medical University, Chongqing, China. E-mail: [superwyy@126.com](mailto:superwyy@126.com)

<sup>d</sup> Department of Urology, Institute of Urology, West China Hospital, Sichuan University, Chengdu, 610041, China. E-mail: [zhliu@scu.edu.cn](mailto:zhliu@scu.edu.cn)

<sup>†</sup> Authors contributed equally to the work.

#### Corresponding author

\*Email: [superwyy@126.com](mailto:superwyy@126.com)

[zhliu@scu.edu.cn](mailto:zhliu@scu.edu.cn)

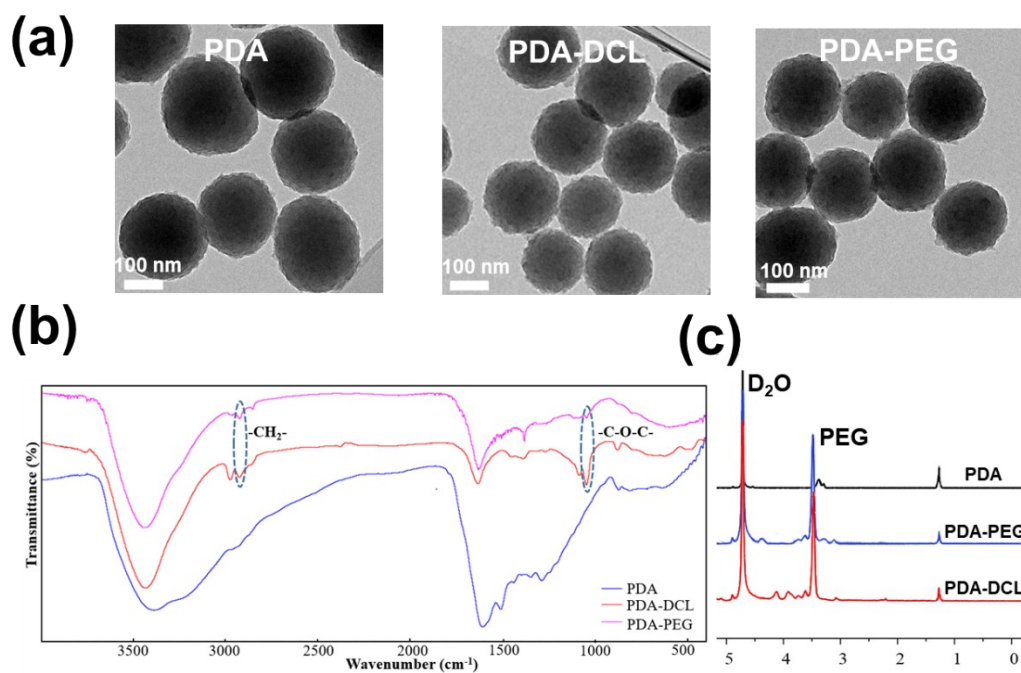


Fig. S1. (a) Transmission electron micrographs of PDA, PDA-DCL, and PDA-PEG nanoparticles. (b) FT-IR spectra of PDA, PDA-DCL, and PDA-PEG nanoparticles. (c) <sup>1</sup>H NMR spectra of PDA, PDA-PEG, and PDA-DCL nanoparticles.

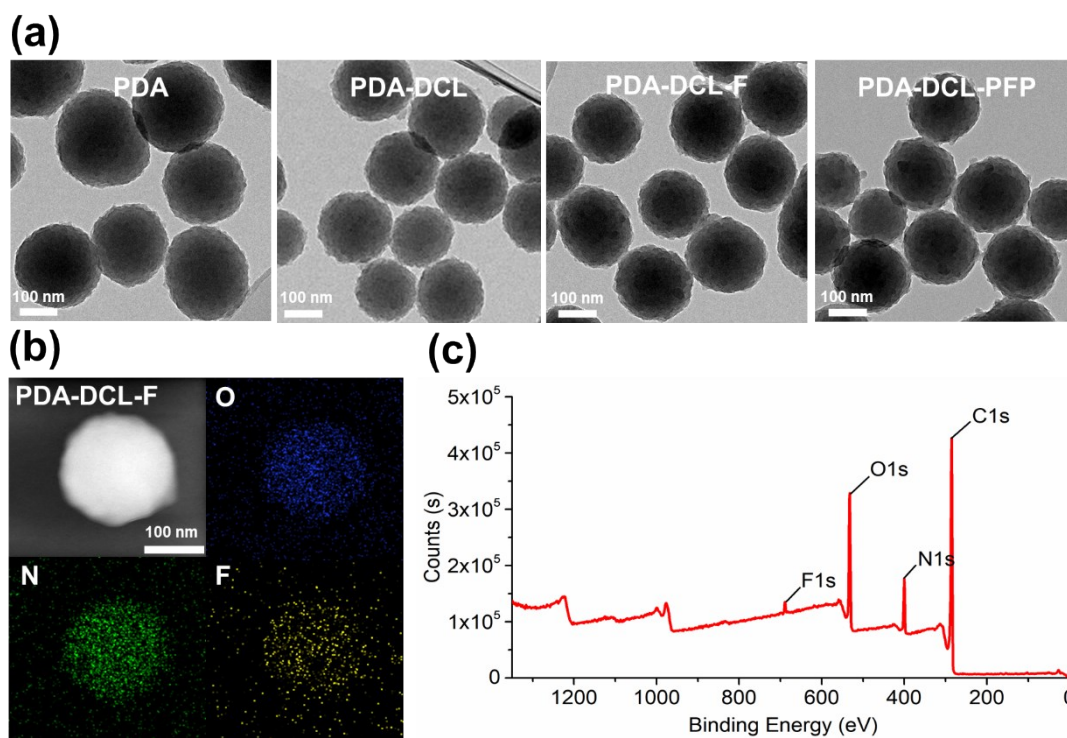


Fig. S2. (a) Transmission electron micrographs of PDA, PDA-DCL, PDA-DCL-F, and PDA-DCL-PFP nanoparticles. (b) Dark-field scanning transmission electron micrograph of a single PDA-DCL-F nanoparticle showing the distribution of O (blue), N (green), and F (yellow). (c) X-ray photoelectron spectrum of PDA-DCL-F nanoparticles.

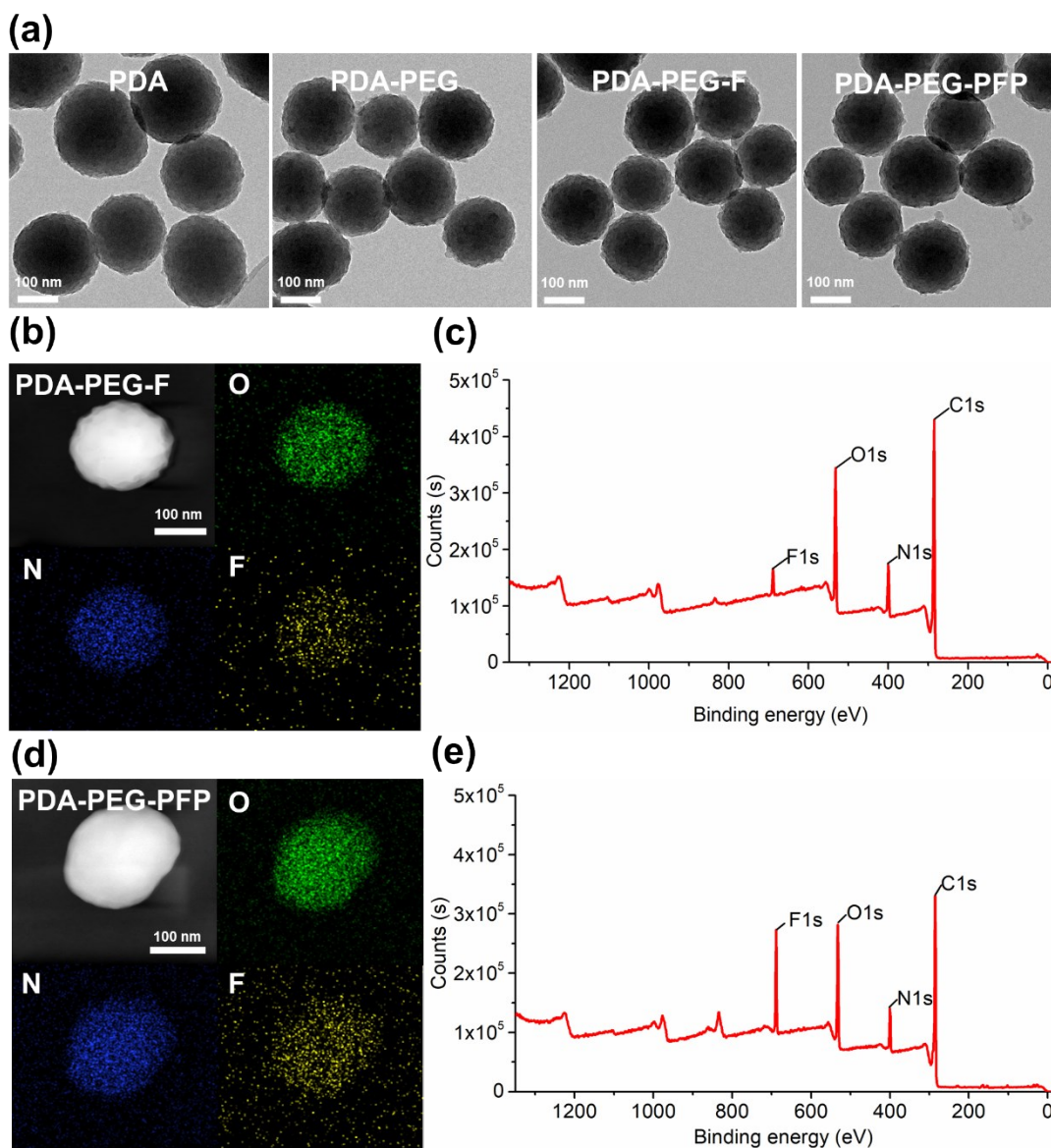


Fig. S3. (a) Transmission electron micrographs of PDA, PDA-PEG, PDA-PEG-F, and PDA-PEG-PFP nanoparticles. (b,d) Dark-field scanning tunneling electron micrographs of single (b) PDA-PEG-F and (d) PDA-PEG-PFP nanoparticles showing the distribution of O (blue), N (green), and F (yellow). (c,e) X-ray photoelectron spectrum of the PDA-PEG-F (c) and PDA-PEG-PFP nanoparticles (e).

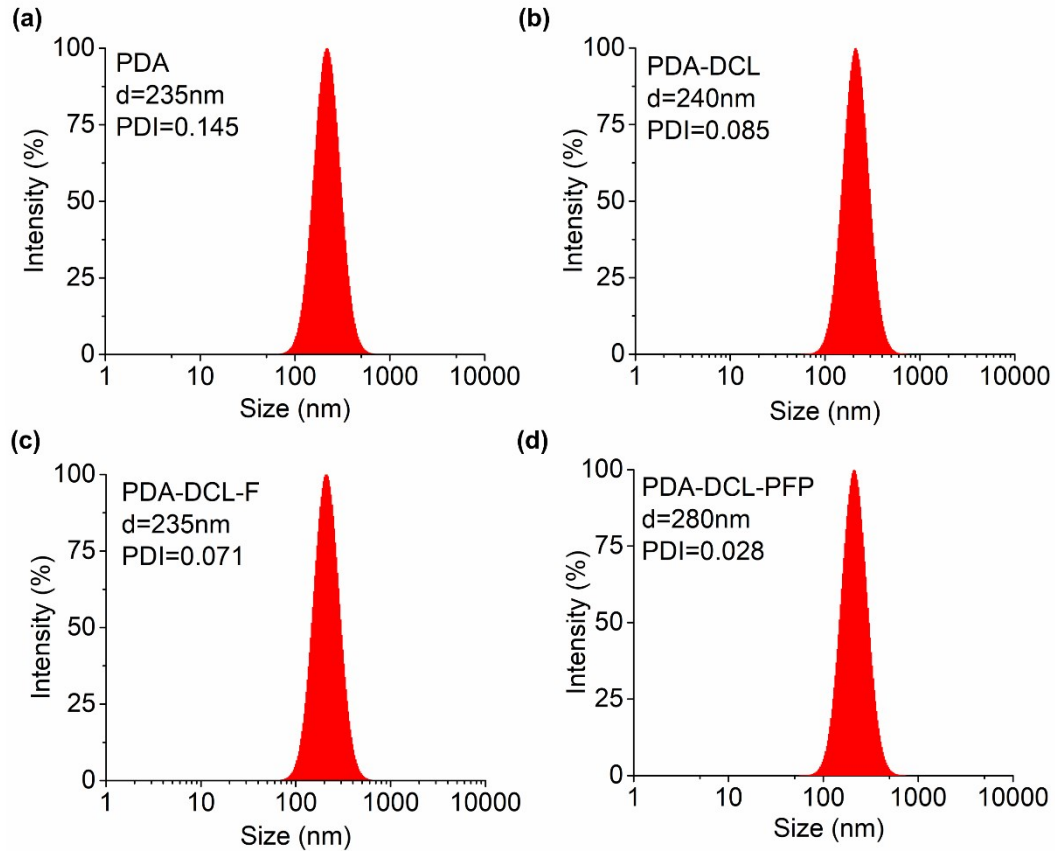


Fig. S4. Size distribution of (a) free PDA, (b) PDA-DCL, (c) PDA-DCL-F, and (d) PDA-DCL-PFP nanoparticles, based on dynamic light scattering.

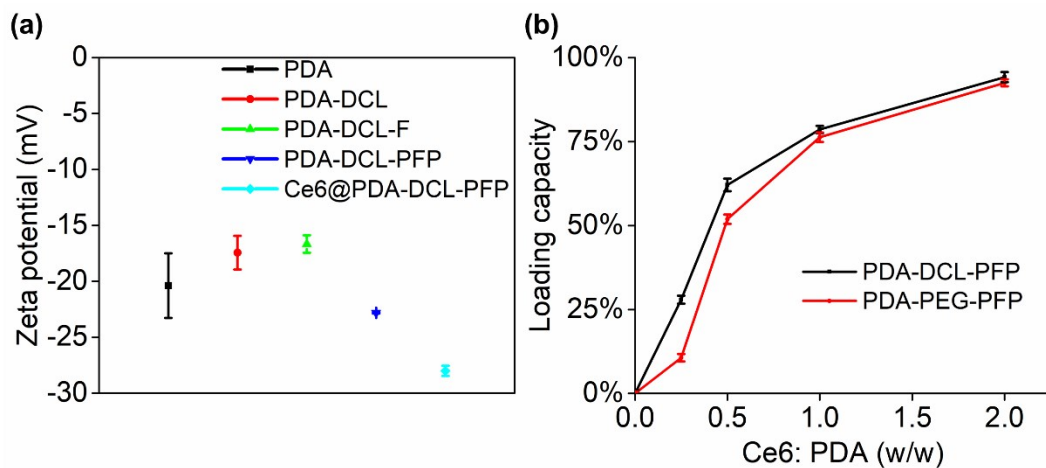


Fig. S5. (a) Zeta potential of the PDA, PDA-DCL, PDA-DCL-F, PDA-DCL-PFP, and Ce6@PDA-DCL-PFP nanoparticles in PBS. (b) Ce6 loading capacities of the PDA-DCL-PFP nanoparticles prepared at different ratios of Ce6 to PDA-DCL-PFP.

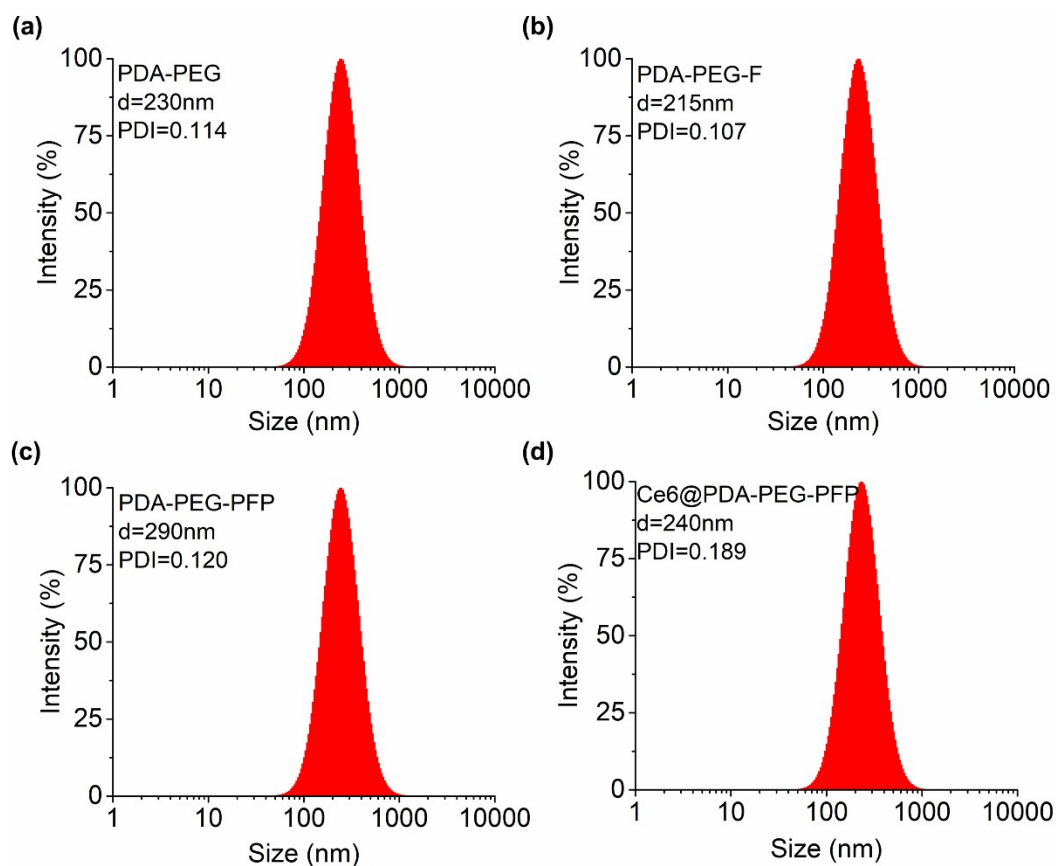


Fig. S6. Size distribution of the (a) PDA-PEG, (b) PDA-PEG-F, (c) PDA-PEG-PFP, and (d) Ce6@PDA-PEG-PFP nanoparticles, based on dynamic light scattering.

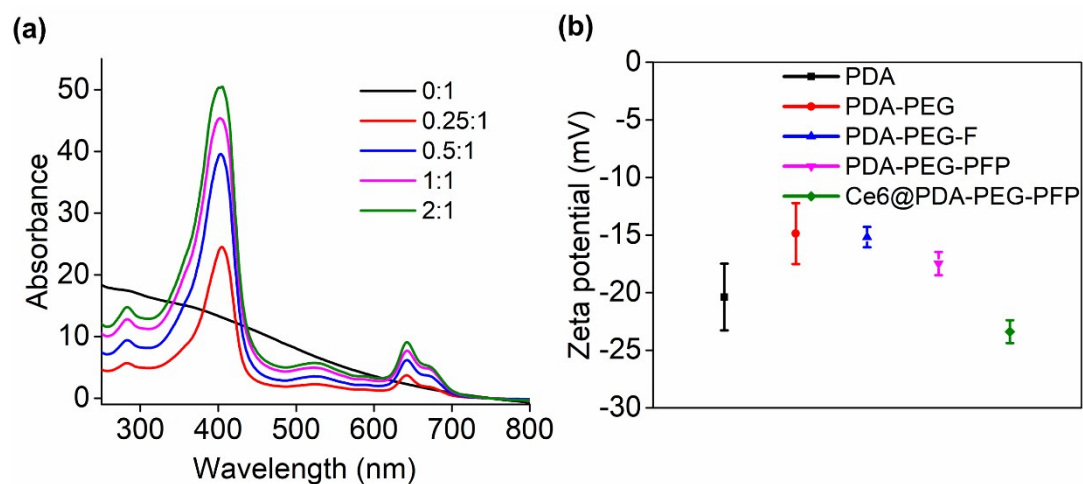


Fig. S7. (a) UV-Vis spectra of Ce6@PDA-PEG-PFP prepared at different ratios of Ce6 to PDA-PEG-PFP. (b) Zeta potential of PDA, PDA-PEG, PDA-PEG-F, PDA-PEG-PFP, and Ce6@PDA-PEG-PFP nanoparticles in PBS.

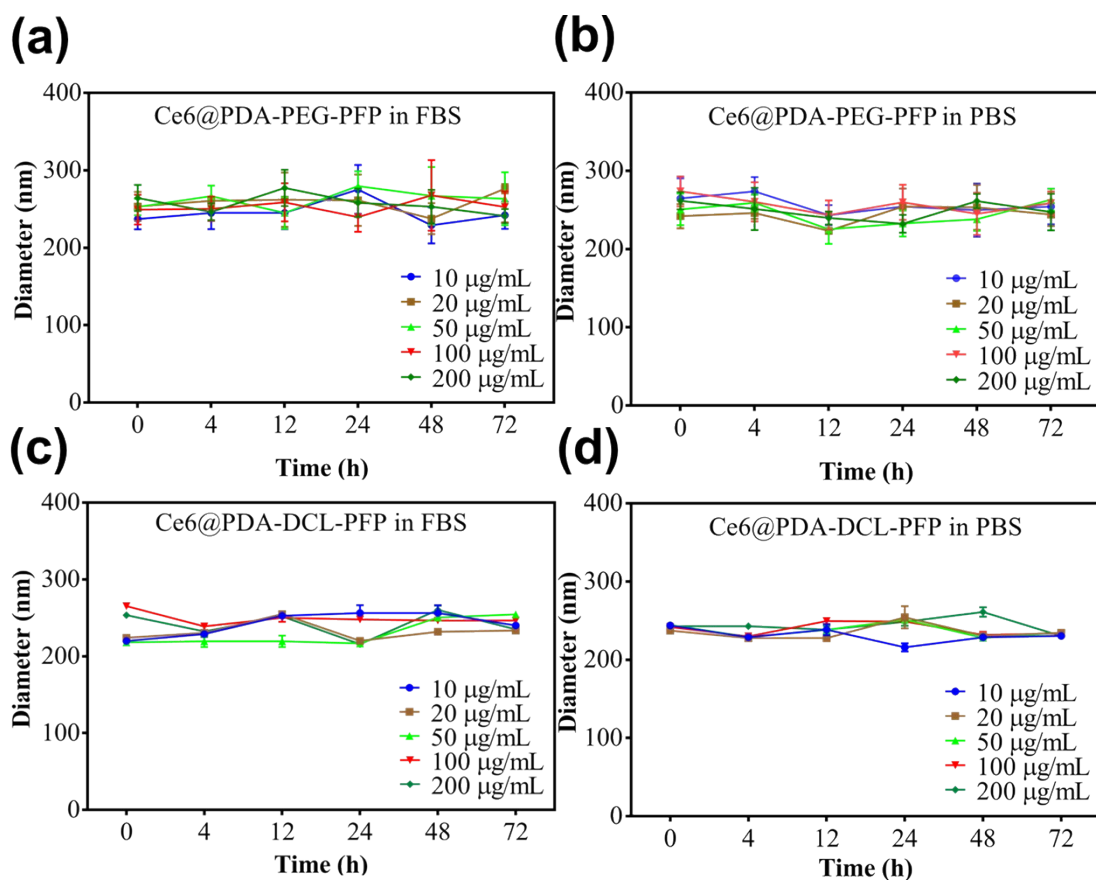


Fig. S8. Diameters of (a,b) Ce6@PDA-PEG-PFP and (c,d) Ce6@PDA-DCL-PFP nanoparticles after incubation at different concentrations for different periods in cell culture medium (10% FBS) or PBS.

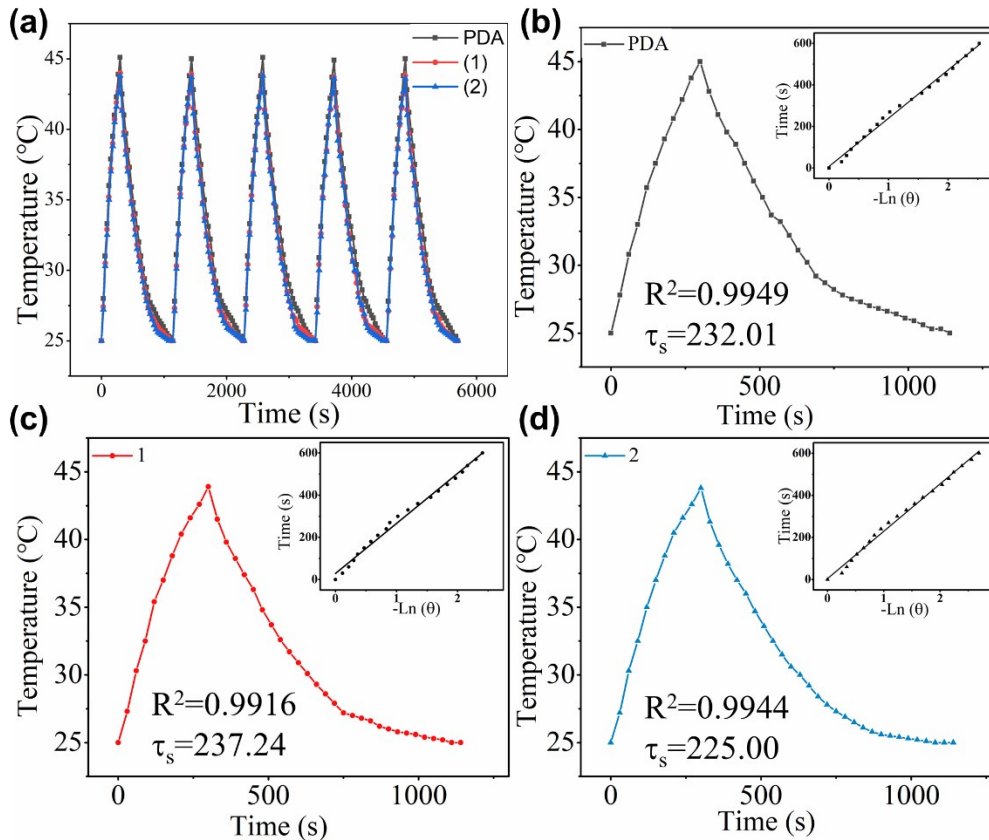


Fig. S9. (a) Temperature curves of PDA, Ce6@PDA-DCL-PFP (1), and Ce6@PDA-PEG-PFP (2) nanoparticles under five on/off cycles of laser irradiation. (b-d) Temperature change of PDA (b), Ce6@PDA-DCL-PFP (c), Ce6@PDA-PEG-PFP (d) under 300 s laser irradiation (808 nm, 1.5 W/cm<sup>2</sup>), respectively, followed by natural cooling. (Insert: linear time data *versus*  $-\ln \theta$  obtained from the cooling period.)

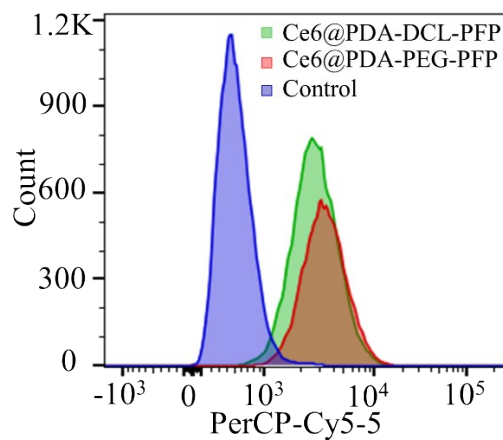


Fig. S10. The cellular internalization of Ce6@PDA-DCL-PFP and Ce6@PDA-PEG-PFP nanoparticles by PSMA-negative PC3 cells revealed by flow cytometry.



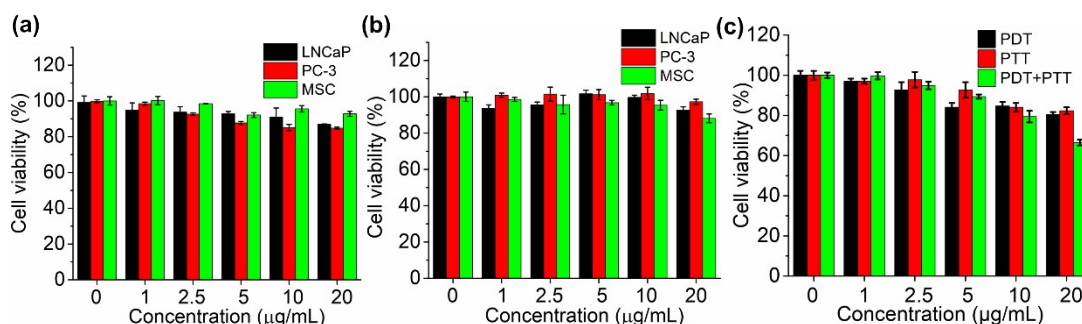


Fig. S11. (a-b) Cell viability of PSMA-positive LNCaP, PSMA-negative PC-3, and nonmalignant MSC cells treated for 24 h with different concentrations of Ce6@PDA-DCL-PFP (a) or Ce6@PDA-PEG-PFP (b). (c) Cell viability of PSMA-negative PC3 cells treated with Ce6@PDA-DCL-PFP under PDT (660 nm, 5 mW/cm<sup>2</sup> for 5 min), PTT (808 nm, 90 mW/cm<sup>2</sup> for 5 min) or both.

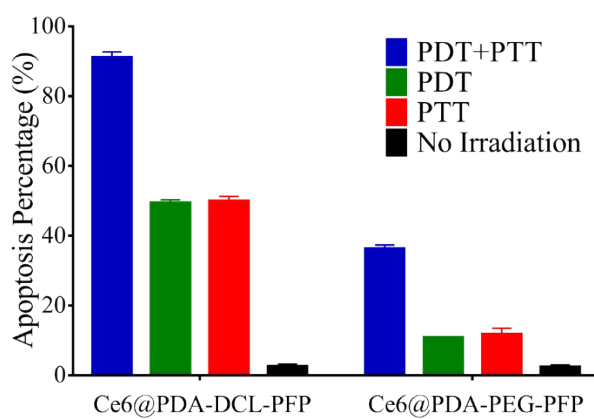


Fig. S12. The apoptotic effect of Ce6@PDA-DCL-PFP and Ce6@PDA-PEG-PFP nanoparticles under various irradiation conditions (no irradiation, PDT, PTT and both).

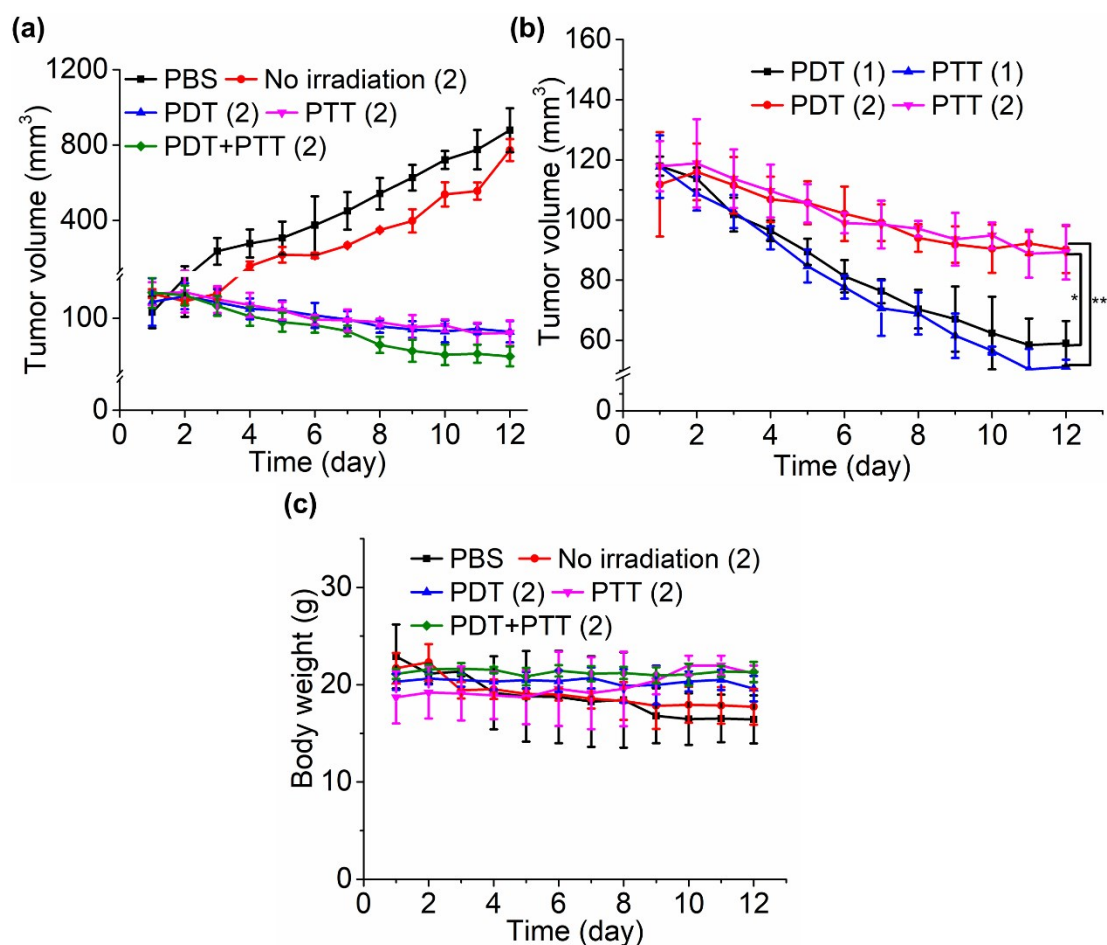


Fig. S13. (a) Tumor growth curves in LNCaP-bearing mice ( $n = 3$ ) during 12 days of treatment with Ce6@PDA-DCL-PFP (group 1) or Ce6@PDA-PEG-PFP (group 2) nanoparticles under various conditions. (b) Comparison of therapeutic effect between Ce6@PDA-DCL-PFP (group 1) and Ce6@PDA-PEG-PFP (group 2) nanoparticles under the same irradiation condition. (c) Body weight changes of mice in different groups during the whole therapy process of Ce6@PDA-PEG-PFP (group 2). Note: (1) and (2) were used to represent the groups treated by Ce6@PDA-DCL-PFP and Ce6@PDA-PEG-PFP nanoparticles, respectively.